

# Naturally Rolled-Up C/Si/C Trilayer Nanomembranes as Stable Anodes for Lithium-Ion Batteries with Remarkable Cycling Performance\*\*

Junwen Deng, Hengxing Ji, Chenglin Yan,\* Jiaxiang Zhang, Wenping Si, Stefan Baunack, Steffen Oswald, Yongfeng Mei, and Oliver G. Schmidt

Lithium-ion batteries (LIBs) have attracted considerable interest because of their wide range of environmentally friendly applications, such as portable electronics, electric vehicles (EVs), and hybrid electric vehicles (HEVs).<sup>[1–5]</sup> For the next generation of LIBs with high energy and high power density, improvements on currently used electrode materials are urgently needed.<sup>[6–10]</sup> Among various anode materials, Si has been extensively studied owing to its highest theoretical capacity (4200 mA h g<sup>−1</sup>), abundance in nature, low cost, and nontoxicity. However, Si-based anodes are notoriously plagued by poor capacity retention resulting from large volume changes during alloy/de-alloy processes (400 %). The intrinsic strain generated during such expansion and contraction easily leads to electrode pulverization and capacity fading. Thus, it is a big challenge to achieve both excellent cyclability and enhanced capacity of Si-based anode materials.

Significant efforts have been devoted to circumvent this issue caused by the volume change of silicon.<sup>[11–15]</sup> Recently, a number of Si nanostructures, including nanoparticles,<sup>[15,16]</sup> nanowires/nanorods,<sup>[17–19]</sup> nanotubes,<sup>[20]</sup> and porous nanostructures<sup>[21,22]</sup> as well as their composites,<sup>[23]</sup> have been fabricated to achieve improved cycling performance.

Among them, tubular structures, with extra interior space for electron and ion transport, as well as for accommodating volume changes, are one of the most attractive and promising configurations for LIBs. However, such anode materials are still far from commercialization, and new strategies for the synthesis of novel structures with superior cycling performance and stability are still much sought-after.

Herein, we report a new tubular configuration made from naturally rolled-up C/Si/C trilayer nanomembranes, which exhibits a highly reversible capacity of approximately 2000 mA h g<sup>−1</sup> at 50 mA g<sup>−1</sup>, and approximately 100 % capacity retention at 500 mA g<sup>−1</sup> after 300 cycles. The sandwich-structured C/Si/C composites, with moderate kinetic properties toward Li<sup>+</sup> ion and electron transport, are of the highest quality. The excellent cycling performance is related to the thin-film effect combined with carbon coating, which play a structural buffering role in minimizing the mechanical stress induced by the volume change of Si. The energy reduction in C/Si/C trilayer nanomembranes after rolling up into multi-winding microtubes results in a significantly reduced intrinsic strain, which can improve capacity and cycling performance. This synthetic process could be compatible with existing industrial sputtering deposition processes as well as roll-to-roll thin-film fabrication technology.

The strategy for the self-release of C/Si/C trilayer nanomembranes using rolled-up nanotechnology<sup>[24]</sup> to form multi-layer C/Si/C microtubes is shown in Scheme 1. First, a sacrificial layer (red color, photoresist ARP 3510) was deposited on top of the Si substrates by spin-coating, then trilayer C/Si/C (10/40/10 nm, respectively) nanomembranes were sequentially deposited by radio frequency sputtering, during which the intrinsic strain caused by thermal expansion effects was generated. When the sacrificial layer was selectively under-

[\*] J. W. Deng, Dr. C. L. Yan, J. Zhang, W. Si, Dr. S. Baunack, Prof. O. G. Schmidt  
Institute for Integrative Nanosciences, IFW Dresden  
Helmholtzstrasse 20, 01069 Dresden (Germany)  
E-mail: c.yan@ifw-dresden.de

J. W. Deng, W. Si, Prof. O. G. Schmidt  
Material Systems for Nanoelectronics  
Chemnitz University of Technology  
Reichenhainer Strasse 70, 09107 Chemnitz (Germany)

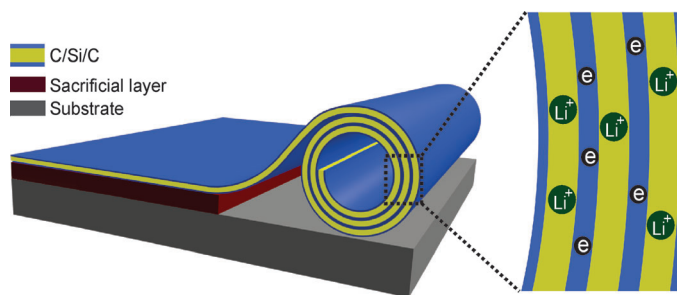
Dr. H. X. Ji  
Department of Materials Science and Engineering  
University of Science and Technology of China  
Hefei, 230036 (P. R. China)

Dr. S. Oswald  
Institute for Complex Materials, IFW Dresden  
Helmholtzstrasse 20, 01069 Dresden (Germany)

Prof. Y. F. Mei  
Department of Materials Science, Fudan University  
Shanghai, 200433 (P. R. China)

[\*\*] This work is financed by the International Research Training Group (IRTG) project and PAKT project "Electrochemical energy storage in autonomous systems, No. 49004401".

Supporting information for this article is available on the WWW under <http://dx.doi.org/10.1002/anie.201208357>.



**Scheme 1.** Fabrication of naturally rolled-up C/Si/C multilayer microtubes.

etched, the composite nanomembranes naturally peeled off from the Si substrates and broke into micrometer-sized pieces owing to the pulling strain, and these pieces further self-rolled into multilayer tubular structures.<sup>[10]</sup> The Si nanomembranes work as the active layer for lithium ion storage, while the carbon layer serves as the supporting layer because of its high stability and excellent conductivity. As a result, the multilayer C/Si/C microtubes exhibited synergistic properties and superior electrochemical performance when used as anodes for LIBs.

The morphology of multilayer C/Si/C microtubes was first characterized by scanning electron microscopy (SEM). Figure 1a shows a top-view image of the electrodes from as-prepared C/Si/C rolled-up tubes with an average diameter of

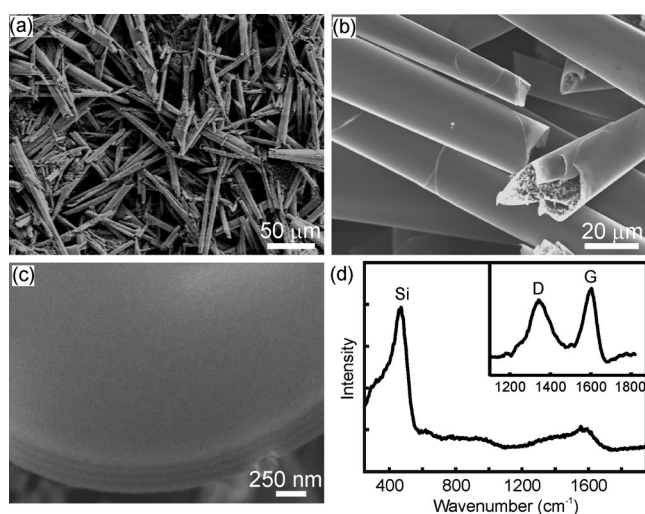


**Figure 1.** SEM images of rolled-up tubes after electrode preparation and a Raman spectrum analysis. a,b) The naturally rolled-up tubes keep their tubular structure after the rigorous electrode fabrication process, indicating an excellent mechanical stability. c) A cross-section of a single tube that prepared by focused ion beam (FIB) cutting, where tightly wrapped windings are visible. d) Micro-Raman spectrum of a single C/Si/C multilayer microtube. Inset: the ID/IG ratio of 0.83, which was obtained from the Trivista Raman spectrometer with higher resolution.

approximately 20  $\mu\text{m}$ . The well-maintained tubular structure suggests excellent mechanical stability of the rolled-up multilayers (Figure 1b). SEM also reveals the structure profile of a single rolled-up multilayer C/Si/C microtube (Figure 1c), which has a hollow inside and layered windings. Raman spectroscopy (InVia, Renishaw) was performed to determine the composition of as-prepared samples at a wavelength of 442 nm (Figure 1d). The broad peak located at  $467\text{ cm}^{-1}$  is related to a typical vibration mode of amorphous silicon, and a peak around  $520\text{ cm}^{-1}$ , indicative of crystalline silicon, was not detected.<sup>[20]</sup> For a Raman spectrum of carbon, it is known that the graphite G-band is located at about  $1580\text{ cm}^{-1}$  and the D-band is near  $1350\text{ cm}^{-1}$ . As shown in Figure 1d, the multilayer C/Si/C microtubes exhibit broad D- and G-bands, which correspond to the characteristic bands of amorphous carbon. As shown in the inset of Figure 1d, the multilayer C/Si/C microtubes have a D/G ratio of 0.83, which is indicative

of amorphous carbon in the composite. Thus the deposited nanomembranes were confirmed to be amorphous structures of both silicon and carbon. The amorphous nature of the C/Si/C trilayer nanostructures enables homogenous volume expansion and contraction, further improving the cycling performance.

Cyclic voltammetry was performed in an assembled half-cell at room temperature in a range of 0–2.5 V versus Li/Li<sup>+</sup> at a scanning rate of  $0.2\text{ mVs}^{-1}$  (Figure 2a). The reduction process corresponds to an uptake of lithium ions to the anode,

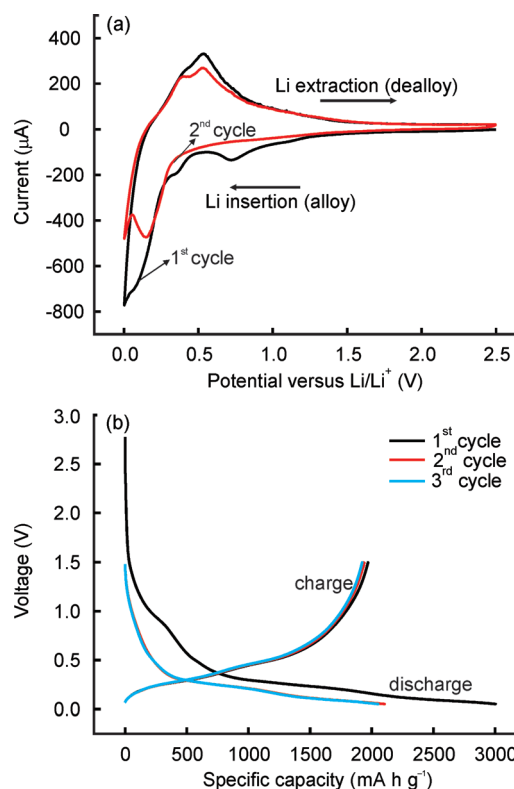


**Figure 2.** a) Cyclic voltammetry curves for the C/Si/C multilayer microtubes from 2.5 V to 0 V versus Li/Li<sup>+</sup> at  $0.2\text{ mVs}^{-1}$  scan rate, the first two cycles are shown; b) Charge-discharge voltage profiles for the C/Si/C multilayer microtubes cycled at a rate of  $50\text{ mA g}^{-1}$  between 1.5 V and 0.05 V versus Li/Li<sup>+</sup>.

while the oxidation process relates to the extraction of lithium ions from the anode. In the first discharge curve, current peaks at around 0.75 V and 0.35 V were assigned to the formation of a solid electrolyte interface (SEI) layer, which disappear in the following cycle and relate to an initial irreversible capacity loss. The different positions of the two peaks are attributed to the different products produced by electrolyte decomposition. The main cathodic peak begins at a potential of around 0.28 V and became quite large below 0.2 V, corresponding to the formation of a series of  $\text{Li}_x\text{Si}$  ( $0 \leq x \leq 4.4$ ) alloys.<sup>[17,25]</sup> The anodic peaks appear at 0.39 V and 0.52 V, corresponding to the phase transition between amorphous  $\text{Li}_x\text{Si}$  to amorphous Si.<sup>[26]</sup> Figure 2b shows the corresponding first three charge/discharge curves in the voltage window of 0.05–1.5 V versus Li/Li<sup>+</sup> at a current density of

50 mA g<sup>-1</sup>. The onset slope at 1.0 V corresponds to the SEI layer formation, which agrees with the CV measurement and disappears in the following cycles. The plateau located at around 0.2 V relates to the alloy formation process between Li and Si.

When employed as anode materials in LIBs, the multilayer C/Si/C microtubes exhibit excellent stability with a highly reversible capacity. Figure 3 shows charge/discharge capacities as a function of cycle number at current densities of 50 mA g<sup>-1</sup> and 500 mA g<sup>-1</sup> in the voltage range of 0.05–1.5 V versus Li/Li<sup>+</sup>, as well as the rate capability at various current rates. The specific reversible capacity of the sample reached approximately 2000 mA h g<sup>-1</sup> at 50 mA g<sup>-1</sup> without discernible decline after ten cycles. Impressively, when cycled at a rate of 500 mA g<sup>-1</sup>, the anode retained its capacity very well for 300

full charge/discharge cycles (Figure 3b). The capacity of the 300th cycle is almost 100% of that of the second one. This outstanding cycling performance benefits from the self-rolling process as well as the unique structural features of the as-prepared multilayer C/Si/C composite structures. First, the C/Si/C tubes are formed by self-winding during film strain release, which could effectively ease the intrinsic strain and offer a minimization of the system energy, thereby enhancing the tolerance to stress cracking caused by the lithiation/delithiation processes. Moreover, this tubular structure provides hollow channels for electrochemical reaction and facilitates fast lithium ion and electron transport. Second, the rolled-up nanomembrane consists of one layer of active Si films and two layers of carbon films to form a novel sandwich nanomembrane, where the double carbon layers provide additional electrical conductivity. Moreover, the softness and the limited volume variation of the carbon materials during reactions firmly surround the inner Si layers and maintain the structural integrity of the system. The sandwiched structures of the membranes provide a stable conductive network and prevent Si pulverization and aggregation during cycling, thus resulting in outstanding cyclability. For a comparison, the rolled-up microtubes made from Si/C bilayer nanomembranes with a similar size show a much lower first-cycle discharge capacity, and the capacity drops quickly at the end of the test (see Supporting Information, Figure S1). Thus, the advantage of the as-prepared rolled-up C/Si/C trilayer nanomembranes for Li<sup>+</sup> ion storage is significant.

The capacity at the current rate of 500 mA g<sup>-1</sup> gradually increases after a slight decrease in the initial ten cycles (Figure 3b). The slight capacity decay results from the SEI layer formation on the exposure surface of the tube inner windings, which are initially tightly wrapped. This phenomenon could be caused by the Si volume changes during cycling, which loose the interior windings and expose the inner surfaces to the electrolyte. The capacity gradually increases afterwards,<sup>[10]</sup> which is mainly due to the activation of the internal wrapped active materials, and finally all of them contribute to the electrochemical reaction. The moderate decrease in capacity starts after 150 cycles, which could be a result of the slight degradation of the electrode during cycling. However, the capacity maintained approximately 1000 mA h g<sup>-1</sup> even after 300 cycles with almost 100% capacity retention. Such ultra-long cycle life is not observed for most other Si-based anodes owing to structure pulverization.

Figure 3c shows the stable rate capability of the multilayer C/Si/C microtubes. It can be seen that the capacity gradually decreases with increasing current density from a low current rate of 0.1 A g<sup>-1</sup> to a high current rate of 25 A g<sup>-1</sup>. Notably, the capacity reversibly recovers to approximately 1000 mA h g<sup>-1</sup> once the current rate goes back to 0.5 A g<sup>-1</sup>. The excellent rate capability of the multilayer C/Si/C microtubes benefits from the strain-released tubular configuration and the double carbon layers that provide improved electrical conductivity along with the mechanical stability.

The evolution of the cross-section morphology of the multilayer microtubes following lithiation was examined.

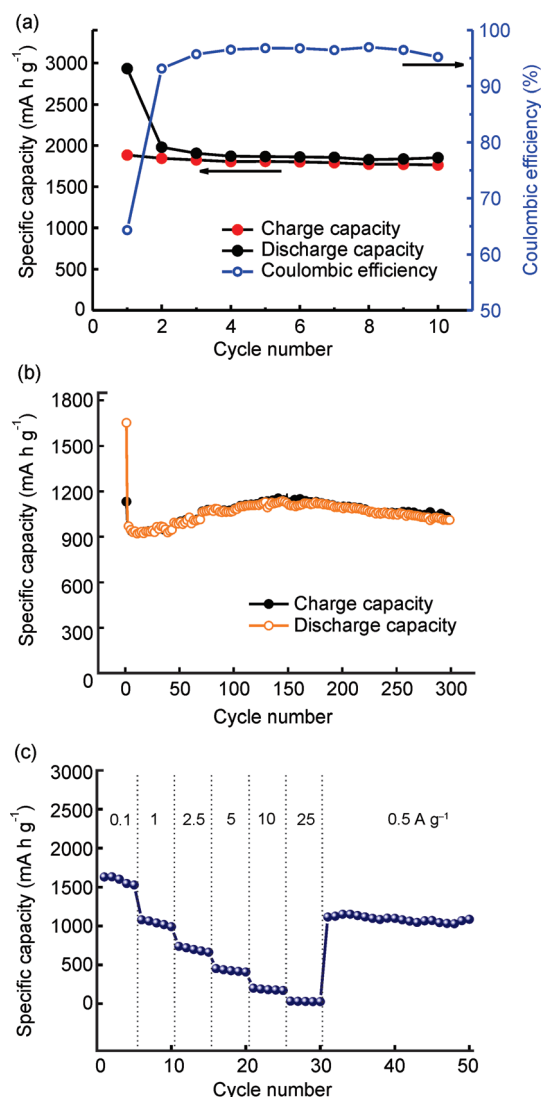


**Figure 3.** Electrochemical characterization for the C/Si/C multilayer microtubes as positive electrodes in LIBs. Cycling performance showing the charge/discharge capacities of the as-prepared multilayer microtubes at current densities of approximately 50 mA g<sup>-1</sup> (a) and 500 mA g<sup>-1</sup> (b) from 0.05 V to 1.5 V versus Li/Li<sup>+</sup>, the capacity was calculated based on the total mass of the C/Si/C microtubes. c) Electrode cycled at various current densities.



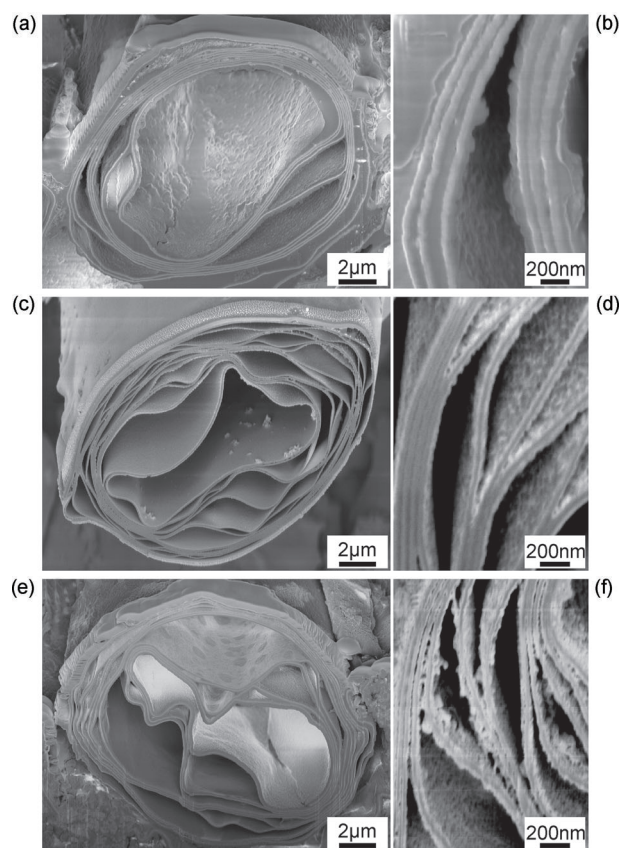


**Figure 4.** Evolution of the morphology of the microtubes after the 1st discharge (a,b), after the 1st charge (c,d), and after the 82nd charge (e,f).

Figure 4a shows the lithiated state relating to the Si-Li alloying process. The surface of the microtubes becomes rough and the layer thickness increased around twice compared with the pristine state. The gaps between the adjacent bilayers of the multilayer C/Si/C microtubes are perhaps due to the volume expansion of Si, which expands towards the hollow interior to accommodate the volume change. Auger electron spectroscopy (AES) sputter depth profiling performed on three different areas of a delithiated C/Si/C microtube revealed a sequential variation of the composition from the outermost layer to the second layer of the C/Si/C microtube (see Supporting Information). This indicates that the carbon coating in the C/Si/C microtubes (with 10 nm carbon coating) does not break during the first delithiation, which is further confirmed by the high-magnification SEM image (Figure S4) and is also consistent with previously reported results.<sup>[27]</sup> After the first charge to 1.5 V, lithium ions were extracted from the  $\text{Li}_x\text{Si}$  alloys, leaving the loosely rolled windings, which could facilitate ion diffusion and electron transport. Mechanical strain generated during lithiation/delithiation easily leads to structure cracking and pulverization, apparently the multilayer C/Si/C microtubes considerably suppress the local stress gradients. Figure 4c indicates that the overall tubular morphology as well as the encapsulation of Si layers within the double carbon layers is well maintained even after 82 cycles, revealing the stable

cycling performance of the multilayer C/Si/C microtubes for lithium ion batteries.

In conclusion, we have produced naturally rolled-up C/Si/C multilayer microtubes for the anode electrodes of LIBs. The electrochemical performance shows significant improvement compared to C/Si and pure Si structure systems. A high capacity of approximately  $2000 \text{ mAh g}^{-1}$  can be retained at a current density of  $50 \text{ mA g}^{-1}$  without discernible decay, and the capacity maintains approximately  $1000 \text{ mAh g}^{-1}$  even after 300 cycles at  $500 \text{ mA g}^{-1}$  with almost 100% capacity retention. Further optimization of the electrode density of the cell is in progress to increase the volumetric capacity values for the purpose of commercialization.<sup>[28]</sup> The enhanced electrochemical performance and excellent cyclability closely relate to the self-rolling technique and the structure design, which have been shown by the cross-sectional images. The naturally strain-released nanomembranes enhance the capability to prevent stress cracking during the electrochemical cycles, and the tubular structures could facilitate fast ion diffusion and electron transport. The sandwiched structure design provides a stable conductive network and prevents Si pulverization and aggregation during cycling, thus guaranteeing superior electrochemical performance.

### Experimental Section

Photoresist ARP 3510 was first spin coated onto a Si wafer substrate as the sacrificial layer, then a 10 nm C film, a 40 nm Si film, and a 10 nm C film were deposited on top sequentially by radio frequency sputtering. The argon pressures for C and Si were  $7.5 \times 10^{-4}$  mbar and  $2 \times 10^{-2}$  mbar, respectively. After under-etching the photoresist by acetone, the tubes were formed automatically with around 20  $\mu\text{m}$  in diameter and several hundred micrometers in length. The bulk tubes were collected after rinsing away the photoresist thoroughly. The morphologies of the as-prepared samples were characterized by scanning electron microscopy (DSM982 Gemini, Carl Zeiss, Oberkochen, Germany). Raman spectroscopy (from Renishaw) was performed with 442 nm wavelength to check the compositions. Auger electron spectroscopy (JAMP 9500, 10 keV, 10 nA) was performed on the delithiated C/Si/C microtube with probe tracking for stage shift compensation.

Swagelok half-cells were assembled in an Ar-filled glove box ( $\text{H}_2\text{O}$ ,  $\text{O}_2 < 0.1$  ppm, Mbraun, Germany). Working electrodes were prepared by mixing the rolled-up tubes with conductive additive carbon black (Timcal) and poly(vinylidene difluoride) (PVDF, Aldrich) binder at a weight ratio of 70:20:10 in *N*-methyl-2-pyrrolidinone (NMP, Aldrich) solvent. The slurry was pasted onto a current collector (Cu foil, Goodfellow) and then dried in a vacuum oven at  $80^\circ\text{C}$  for 10 h. The dried electrode was punched into  $\varnothing = 10$  mm discs for cell assembly. The density of each cell was determined to be around  $0.51 \text{ mg cm}^{-2}$ . Metallic Li foil was used as both the counter and reference electrode, and a glass fiber membrane (Whatman) was used as the separator. The electrolyte consisted of a solution of 1M  $\text{LiPF}_6$  in ethylene carbonate/dimethylcarbonate (EC/DMC; 1:1 by weight; Merck), including 2 wt% vinylene carbonate (VC) electrolyte additive (Merck). Galvanostatic cycling of the assembled cells were carried out with an Arbin instrument BT2000 at a voltage range of 0.05–1.5 V versus  $\text{Li/Li}^+$  at different current densities. The mass ratio of the Si/C was 0.67, which was determined from the thicknesses of the films, the surface area, and the densities of Si ( $d_{\text{Si}} = 2.0 \text{ g cm}^{-3}$ ) and C ( $d_{\text{C}} = 2.0 \text{ g cm}^{-3}$ ) for amorphous Si and C. The capacity in our work was calculated based on the total mass of the C/Si/C microtubes. Cross-sections of the structures after cycling were

characterized by Focus ion beam cutting (CrossBeam Workstation NVision40, Carl Zeiss).

Received: October 17, 2012

Revised: November 28, 2012

Published online: January 22, 2013

**Keywords:** anodes · lithium-ion batteries · nanomembranes · nanotubes · silicon

- [1] J. M. Tarascon, M. Armand, *Nature* **2001**, *414*, 359.
- [2] M. Armand, J. M. Tarascon, *Nature* **2008**, *451*, 652.
- [3] P. G. Bruce, B. Scrosati, J. M. Tarascon, *Angew. Chem.* **2008**, *120*, 2972; *Angew. Chem. Int. Ed.* **2008**, *47*, 2930.
- [4] P. Gibot, M. Casas-Cabanas, L. Laffont, S. Levasseur, P. Carlach, S. Hamelet, J. M. Tarascon, C. Masquelier, *Nat. Mater.* **2008**, *7*, 741.
- [5] B. Key, M. Morcrette, J. M. Tarascon, C. P. Grey, *J. Am. Chem. Soc.* **2011**, *133*, 503.
- [6] M. S. Whittingham, *Chem. Rev.* **2004**, *104*, 4271.
- [7] C. Sun, S. Rajasekhara, J. B. Goodenough, F. Zhou, *J. Am. Chem. Soc.* **2011**, *133*, 2132.
- [8] Y. Yu, L. Gu, C. Zhu, P. A. van Aken, J. Maier, *J. Am. Chem. Soc.* **2009**, *131*, 15984.
- [9] L. Zhou, D. Y. Zhao, X. W. Lou, *Adv. Mater.* **2012**, *24*, 745.
- [10] H. X. Ji, X. L. Wu, L. Z. Fan, C. Krien, I. Fiering, Y. G. Guo, Y. F. Mei, O. G. Schmidt, *Adv. Mater.* **2010**, *22*, 4591.
- [11] H. Zhang, P. V. Braun, *Nano Lett.* **2012**, *12*, 2778.
- [12] R. Teki, M. K. Datta, R. Krishnan, T. C. Parker, T. M. Lu, P. N. Kumta, N. Koratkar, *Small* **2009**, *5*, 2236.
- [13] A. Esmanski, G. A. Ozin, *Adv. Funct. Mater.* **2009**, *19*, 1999.
- [14] H. Wu, G. Chan, J. W. Choi, I. Ryu, Y. Yao, M. T. McDowell, S. W. Lee, A. Jackson, Y. Yang, L. B. Hu, Y. Cui, *Nat. Nanotechnol.* **2012**, *7*, 310.
- [15] H. Kim, M. Seo, M.-H. Park, J. Cho, *Angew. Chem.* **2010**, *122*, 2192; *Angew. Chem. Int. Ed.* **2010**, *49*, 2146.
- [16] H. Wu, G. Y. Zheng, N. Liu, T. J. Carney, Y. Yang, Y. Cui, *Nano Lett.* **2012**, *12*, 904.
- [17] C. K. Chan, H. L. Peng, G. Liu, K. McIlwrath, X. F. Zhang, R. A. Huggins, Y. Cui, *Nat. Nanotechnol.* **2008**, *3*, 31.
- [18] J. W. Choi, J. McDonough, S. Jeong, J. S. Yoo, C. K. Chan, Y. Cui, *Nano Lett.* **2010**, *10*, 1409.
- [19] N. A. Liu, L. B. Hu, M. T. McDowell, A. Jackson, Y. Cui, *ACS Nano* **2011**, *5*, 6487.
- [20] M. H. Park, M. G. Kim, J. Joo, K. Kim, J. Kim, S. Ahn, Y. Cui, J. Cho, *Nano Lett.* **2009**, *9*, 3844.
- [21] B. Hertzberg, A. Alexeev, G. Yushin, *J. Am. Chem. Soc.* **2010**, *132*, 8548.
- [22] Y. Yu, L. Gu, C. B. Zhu, S. Tsukimoto, P. A. van Aken, J. Maier, *Adv. Mater.* **2010**, *22*, 2247.
- [23] A. Magasinski, P. Dixon, B. Hertzberg, A. Kvit, J. Ayala, G. Yushin, *Nat. Mater.* **2010**, *9*, 353.
- [24] O. G. Schmidt, K. Eberl, *Nature* **2001**, *410*, 168.
- [25] M. Green, E. Fielder, B. Scrosati, M. Wachtler, J. S. Moreno, *Electrochem. Solid-State Lett.* **2003**, *6*, A75.
- [26] V. Baranchugov, E. Markevich, E. Pollak, G. Salitra, D. Aurbach, *Electrochem. Commun.* **2007**, *9*, 796.
- [27] H. Liu, J. Y. Huang, *Energy Environ. Sci.* **2011**, *4*, 3844.
- [28] H. T. Nguyen, F. Yao, M. R. Zamfir, C. Biswas, K. P. So, Y. H. Lee, S. M. Kim, S. N. Cha, J. M. Kim, D. Pribat, *Adv. Energy Mater.* **2010**, *22*, 4591.